Job, C., Dietrich, J., Shire, D., Teissère, M., & Job, D. (1987) *Biochem. J. 244*, 151-157.
Job, C., Soulié, J.-M., & Job, D. (1988) *Biochem. J. 252*, 55-63.
Job, D., Marmillot, P., Job, C., & Jovin, T. M. (1988) *Biochemistry 27*, 6371-6378.
Jovin, T. M., Soumpasis, D. M., & McIntosh, L. P. (1987) *Annu. Rev. Phys. Chem. 38*, 521-560.
Kane, C. M. (1988) *Biochemistry 27*, 3187-3196.
Koo, H., Wu, H. M., & Crothers, D. M. (1986) *Nature (London) 321*, 501-506.
Levin, J. R., Krummel, B., & Chamberlin, M. J. (1987) *J. Mol. Biol. 196*, 85-100.
Lippard, S. J. (1987) *Pure Appl. Chem. 59*, 731-742.
Loehrer, P. J., & Einhorn, L. H. (1984) *Ann. Intern. Med. 100*, 704-713.
Maniatis, T., Fritsch, E. F., & Sambrook, J. (1982) in *Molecular Cloning*, pp 150-185, Cold Spring Harbor Laboratory, Cold Spring Harbor, NY.
Marrot, L., & Leng, M. (1989) *Biochemistry 28*, 1454-1461.
McClure, W. R. (1985) *Annu. Rev. Biochem. 54*, 171-204.
Oen, H., & Wu, C. W. (1978) *Proc. Natl. Acad. Sci. U.S.A. 75*, 1778-1782.
Pinto, A. L., & Lippard, S. J. (1985) *Proc. Natl. Acad. Sci. U.S.A. 82*, 4616-4619.
Randerath, K., & Randerath, E. (1967) *Methods Enzymol. A12*, 323-347.
Reedijk, J. (1987) *Pure Appl. Chem. 59*, 181-192.
Rice, J. A., Crothers, D. M., Pinto, A. L., & Lippard, S. J. (1988) *Proc. Natl. Acad. Sci. U.S.A. 85*, 4158-4161.
Rosenberg, B., Van Camp, L., Trosko, J. E., & Mansour, V. H. (1969) *Nature (London) 222*, 385-386.
Sawadogo, M., & Sentenac, A. (1990) *Annu. Rev. Biochem. 59*, 711-754.
Schwartz, A., Marrot, L., & Leng, M. (1989) *Biochemistry 28*, 7975-7979.
Schwartz, A., Sip, M., & Leng, M. (1990) *J. Am. Chem. Soc. 112*, 3673-3674.
Sorenson, C. M., & Eastman, A. (1988a) *Cancer Res. 48*, 4484-4488.
Sorenson, C. M., & Eastman, A. (1988b) *Cancer Res. 48*, 6703-6707.
Sylvester, J. E., & Cashel, M. (1980) *Biochemistry 19*, 1069-1074.
Van Houten, B. (1990) *Microbiol. Rev. 54*, 18-51.
Villani, G., Hübscher, U., & Butour, J.-L. (1988) *Nucleic Acids Res. 16*, 4407-4418.
von Hippel, P. H., Bear, D. G., Morgan, W. D., & McSwiggen, J. A. (1984) *Annu. Rev. Biochem. 53*, 389-446.

Hematoporphyrin-Promoted Photoinactivation of Mitochondrial Ubiquinol-Cytochrome *c* Reductase: Selective Destruction of the Histidine Ligands of the Iron–Sulfur Cluster and Protective Effect of Ubiquinone†

Toshiaki Miki, Linda Yu, and Chang-An Yu*
Department of Biochemistry, OAES, Oklahoma State University, Stillwater, Oklahoma 74078
Received January 30, 1990; Revised Manuscript Received August 15, 1990

ABSTRACT: Purified ubiquinol-cytochrome *c* reductase of beef heart mitochondria is very stable in aqueous solution; it suffers little damage upon illumination with visible light under aerobic or anaerobic conditions. However, it is rapidly inactivated when the photosensitizer hematoporphyrin is present during illumination. The hematoporphyrin-promoted photoactivation is dependent on sensitizer dose, illumination time, and oxygen. Singlet oxygen is shown to be the destructive agent in this system. The photoinactivation of ubiquinol-cytochrome *c* reductase is prevented by excess exogenous ubiquinone, regardless of its redox state. This protective effect is not due to protein–ubiquinone interactions but to the singlet oxygen scavenger property of ubiquinone. Ubiquinone also protects against hematoporphyrin-promoted photoinactivation of succinate-ubiquinone reductase and cytochrome *c* oxidase. The photoinactivation site in ubiquinol-cytochrome *c* reductase is the iron–sulfur cluster of Rieske's protein. Two histidine residues, presumably serving as two ligands for the iron–sulfur cluster of Rieske's protein, are destroyed. No polypeptide bond cleavage is detected. Photoinactivation has little effect on the spectral properties of cytochromes *b* and c_1 but alters their reduction rates substantially. This photoinactivation also causes the formation of proton-leaking channels in the complex. When the photoinactivated reductase is co-inlaid with intact ubiquinol-cytochrome *c* reductase or cytochrome *c* oxidase in a phospholipid vesicle, no proton ejection can be detected during the oxidation of their corresponding substrates.

Ubiquinol-cytochrome *c* reductase (commonly known as cytochrome b–c_1 complex or complex III) is a segment of the mitochondrial respiratory chain which catalyzes antimycin-sensitive electron transfer from ubiquinol to cytochrome *c* (Rieske, 1986). The redox components in this complex are two *b* cytochromes (*b*-565 and *b*-562), one *c*-type cytochrome (c_1), one-high potential iron–sulfur cluster (2Fe-2S Rieske center), and a ubiquinone. The complex contains 7–11 protein subunits depending on the sodium dodecyl sulfate–polyacrylamide gel electrophoresis (SDS–PAGE)[1] systems used

† This work was supported by a grant from the National Institutes of Health (GM 30721).

[1] Abbreviations: ISP, iron–sulfur protein; Q_2, 2,3-dimethoxy-5-methyl-6-geranyl-1,4-benzoquinone; Q_2H_2, 2,3-dimethoxy-5-methyl-6-geranyl-1,4-benzoquinol; QCR, ubiquinol-cytochrome *c* reductase; SDS–PAGE, sodium dodecyl sulfate–polyacrylamide gel electrophoresis.

0006-2960/91/0430-230$02.50/0

(Yu et al., 1974; Bell & Capaldi, 1976; Gellerfors & Nelson, 1977; Schägger et al., 1986; Gonzalez-Halphen et al., 1988). The electron transfer and proton translocation mechanisms, as well as the spatial arrangement of this complex in the membrane, have been the subjects of intensive investigation (Mitchell, 1976; Wikström et al., 1981; Hatefi, 1985; Gonzalez-Halphen et al., 1988). Electron transfer by this complex is coupled with the translocation of protons across the mitochondrial inner membrane to generate a proton gradient and membrane potential. Although the proposed Q-cycle (Mitchell, 1976) mechanism for the electron transfer path in this complex can explain most of experimental data, some results (Tsai et al., 1987) cannot be explained by this scheme. The redox-linked proton pumping (Papa et al., 1982) mechanism has recently gained support over the direct ligand conduct proton translocation advocated by the Q-cycle mechanism. The mechanism of proton translocation in this complex remains to be clarified.

The use of specific inhibitors (von Jagow & Link, 1986) and of resolution and reconstitution (Schägger et al., 1986; Shimomura et al., 1984; Trumpower & Edwards, 1979) in the study of electron and proton transfer mechanisms has been quite successful. Selective destruction of one or more of the redox centers in a complex has some advantages over the resolution and reconstitution approach since it may eliminate the complication arising from the uncertainty of the "structural contribution" of the apoprotein of the redox component of interest. For example, if the removal of the iron–sulfur protein diminishes proton translocation activity of ubiquinol-cytochrome *c* reductase, one cannot tell whether this loss is due to the iron–sulfur cluster alone or to the apoprotein as well. By selective destruction of a redox prosthetic group and determination of the partial electron transfer reactions in the damaged complex, the role of the apoprotein of the damaged redox component in the electron transfer reactions can be assessed. Similarly, the role of the apoprotein of the destroyed redox component in proton translocation can be assessed by measuring proton ejection activity of phospholipid vesicles inlaid with the damaged complex alone or together with another proton-ejecting complex.

Recently we found that ubiquinol-cytochrome *c* reductase is inactivated when illuminated with a projector light in the presence of hematoporphyrin under aerobic conditions. Photoinactivation is proportional to the degree of destruction of the iron–sulfur cluster in the complex, indicating that this is the site destroyed by hematoporphyrin-activated singlet oxygen (Spikes & Machnight, 1971; Bourdon & Durante, 1971). The oxidation of histidine residues leading to the destruction of the iron–sulfur cluster is consistent with the idea that the N-atom of the imidazole group of the histidine residues serves as two ligands of the iron–sulfur cluster (Cline et al., 1985; Telser et al., 1987; Gurbiel et al., 1989). The photoinactivated complex forms a proton-leaking vesicle when reconstituted with phospholipids. When the photoinactivated reductase complex is co-inlaid with intact reductase or other proton-pumping complexes in the phospholipid vesicles, a decrease in the proton ejection activity of the proton pumping complex was observed. These findings add a new dimension to the examination of the role of the iron–sulfur protein in electron and proton transfer reactions. Mitochondrial ubiquinol-cytochrome *c* reductase has been reported to be partially sensitive to blue light, and some destruction of cytochrome has been observed during prolonged illumination (Ninnemann et al., 1970). The photoinactivation of ubiquinol-cytochrome *c* reductase in the absence of a photosensitizer is apparently different from that which occurs in the presence of hematoporphyrin. In the latter, a singlet oxygen is the key destructive agent as the inactivation is prevented by singlet oxygen scavengers. Addition of ubiquinone prevents the hematoporphyrin-promoted photoinactivation. Herein we report the nature of, conditions for, and effect of ubiquinone on the hematoporphyrin-promoted photoinactivation of ubiquinol-cytochrome *c* reductase.

Materials and Methods

Materials. Cholate, horse cytochrome *c*, type III, and hematoporphyrin were from Sigma; 2,2,6,6-tetramethyl-4-piperidone hydrochloride and 2,5-dimethylfuran were from Aldrich. Bovine heart ubiquinol-cytochrome *c* reductase and its Q- and phospholipid-depleted forms were prepared and assayed as previously reported (Yu & Yu, 1980). Iron–sulfur protein was prepared according to the method reported by Shimomura et al. (1986). 2,3-Dimethoxy-5-methyl-6-geranyl-1,4-benzoquinone (Q_2) and its reduced form (Q_2H_2) were synthesized according to methods (Yu & Yu, 1982) previously described. Asolectin was obtained from Associate Concentrate and purified according to the method of Kagawa and Racker (1971). The concentrations of cytochromes *b* and c_1 were determined spectrophotometrically (Yu & Yu, 1980). Hematoporphyrin was dissolved in 0.1 N KOH and then neutralized with 1 N HCl. Potassium phosphate buffer, pH 7.4, was added to a final concentration of 50 mM, and the concentration of hematoporphyrin was estimated spectrophotometrically with a molar extinction coefficient of 1.4×10^5 $M^{-1} \cdot cm^{-1}$ at 391 nm (Blum & Grossweiner, 1985). Amino acid compositions of isolated iron–sulfur protein and ubiquinol-cytochrome *c* reductase were determined by HPLC with a C-18 column according to the method of Heinrikson and Meredith (1984). The duplicated protein samples were hydrolyzed with 6 N HCl for 12, 24, and 36 h at 110 °C under an argon atmosphere. SDS–PAGE was carried out by the method of Laemmli (1970). The amino acid composition of the iron–sulfur protein in ubiquinol-cytochrome *c* reductase was determined from the protein band sliced from the unstained gel of SDS–PAGE, the stained gel being used as a marker. The protein in gel slices was eluted electrophoretically before it was subjected to hydrolysis with 6 N HCl.

Illumination of Ubiquinol-Cytochrome c Reductase in the Presence of Hematoporphyrin. Aliquots of 0.5 mL of ubiquinol-cytochrome *c* reductase, 2 μM cytochrome c_1 or otherwise as specified, in 50 mM potassium phosphate buffer, pH 7.4, containing 0.25% potassium cholate, were mixed with the indicated concentrations of hematoporphyrin. The samples were illuminated in a glass test tube with a 110-V, 600-W slide projector (Kodak Model 550) at a distance of 15 cm at room temperature for various periods of time. Photoinactivation of purified iron–sulfur protein was carried out under the same conditions except the protein concentration used was 0.5 mg/mL.

Spectrophotometric measurements were carried out in a SLM-Aminco dual-wavelength spectrophotometer, Model DW 2000, at room temperature. EPR measurements were performed in a Bruker ER200D spectrometer. The instrument settings are given in the figure legends.

Results and Discussion

Effect of Hematoporphyrin Concentration, Illumination Time, and Oxygen on Photoinactivation of Ubiquinol-Cytochrome c Reductase. Figure 1 shows the hematoporphyrin concentration-dependent illumination time dependent, and oxygen-dependent photoinactivation of ubiquinol-cytochrome

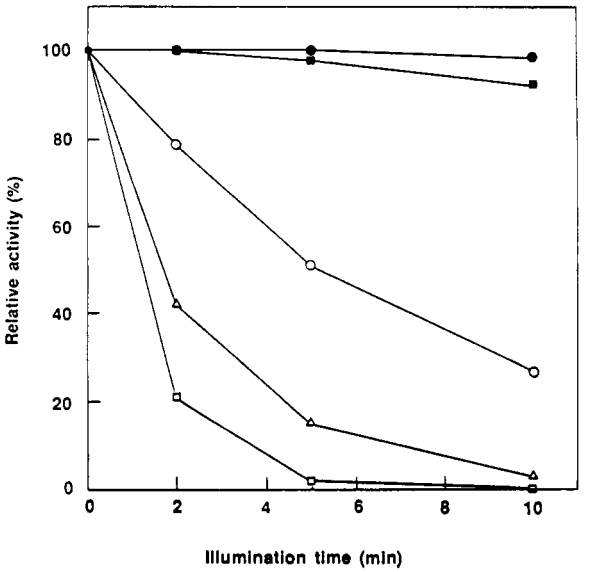

FIGURE 1: Effect of illumination time, hematoporphyrin concentration, and oxygen on photoinactivation of ubiquinol-cytochrome *c* reductase: 0.5-mL aliquots of ubiquinol-cytochrome *c* reductase, 0.3 μM cytochrome c_1, in 50 mM potassium phosphate buffer, pH 7.4, containing 0.25% sodium cholate and 0 (●), 1.5 (○), 3.0 (△), 15.2 (□, ■) μM hematoporphyrin were illuminated with a slide projector light at different lengths of time under aerobic (●, ○, △, □) and anaerobic (■) conditions. At the times indicated, ubiquinol-cytochrome *c* reductase activity of each sample was assayed. The 100% activity represents 15 μmol of cytochrome *c* reduced per minute per nanomole of cytochrome c_1.

c reductase. Purified ubiquinol-cytochrome *c* reductase suffers no loss of activity when illuminated with slide projector light for 10 min at room temperature under aerobic (Figure 1, curve with solid circles) or anaerobic (data not shown) conditions in the absence of hematoporphyrin. However, when illuminated for different lengths of time under aerobic conditions in the presence of various concentrations of hematoporphyrin, inactivation increases with the concentration of hematoporphyrin and the illumination time. A 5-min illumination of ubiquinol-cytochrome *c* reductase in the presence of 1.5, 3.0, and 15.2 μM hematoporphyrin results in a loss of 49%, 84%, and 98% of the activity, respectively. When ubiquinol-cytochrome *c* reductase is illuminated in the presence of 15.2 μM hematoporphyrin under aerobic conditions, no loss in activity is observed (Figure 1, curve with solid squares). This suggests that, in addition to photosensitizer, oxygen also plays an essential role in the photoinactivation.

The photoinactivation of ubiquinol-cytochrome *c* reductase in the presence of hematoporphyrin is different from that reported for complex III (Ninnemann et al., 1970). The time required for the maximum hematoporphyrin-promoted photoinactivation of ubiquinol-cytochrome *c* reductase is very short, only a few minutes. However, it took hours of illumination to show inactivation in the absence of photosensitizer (Ninnemann et al., 1970). Clearly, hematoporphyrin acts as a photosensitizer.

Involvement of Singlet Oxygen in Hematoporphyrin-Promoted Photoinactivation of Ubiquinol-Cytochrome c Reductase. Since the hematoporphyrin-promoted photoinactivation of ubiquinol-cytochrome *c* reductase occurs only under aerobic conditions, the destructive agent cannot be photoactivated hematoporphyrin. Rather, it must be activated oxygen. The formation of activated oxygen during illumination of hematoporphyrin was established by noting the formation of a stable nitroxide radical in the presence of an activated oxygen trap, 2,2,6,6-tetramethyl-4-piperidone (Moan & Wold, 1979).

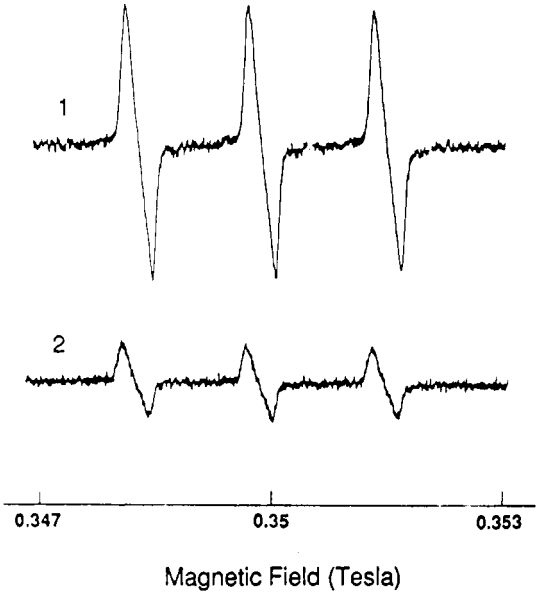

FIGURE 2: Nitroxide radical formed by 2,2,6,6-tetramethyl-4-piperidone during the illumination of hematoporphyrin in the presence and absence of ubiquinone-2. EPR spectra: To 0.5 mL of 50 mM potassium phosphate buffer, pH 7.4, containing 0.25% sodium cholate, 50 mM 2,2,6,6-tetramethyl-4-piperidone, and 15.7 μM hematoporphyrin was added 2.5 μL of 95% ethanolic solution containing (1) 0 and (2) 5 mM Q_2H_2; illumination was for 10 min. The illuminated samples were placed in a flat quartz cell, and EPR spectra were recorded at room temperature. The instrument settings were as follows: field modulation frequency, 100 kHz; microwave frequency, 9.76 GHz; modulation amplitude, 3.2 G; microwave power, 2 mW; time constant, 0.2 s.

Table I: Effect of 2,5-Dimethylfuran and Superoxide Dismutase on the Hematoporphyrin-Promoted Photoinactivation of Ubiquinol-Cytochrome *c* Reductase

addition	inactivation (%)
none	98
2,5-dimethylfuran	12
superoxide dismutase	95

Spectrum 1 of Figure 2 shows EPR characteristics of the stable nitroxide radical generated by the illumination of hematoporphyrin in buffer. The concentration of nitroxide radical increases almost linearly with the duration of illumination. The formation of nitroxide radical is suppressed by about 60% by the presence of 5 mM ubiquinone-2 (Q_2H_2) in the system. These results clearly demonstrate that activated oxygen is involved in the hematoporphyrin-promoted inactivation of ubiquinol-cytochrome *c* reductase. However, there are two species of activated oxygen available in the photosensitizer-activated system: one is singlet oxygen; the other is superoxide ion. It is important to identify the activated oxygen species responsible for photoinactivation.

If singlet oxygen is the destructive agent, the addition of 2,5-dimethylfuran, a singlet oxygen scavenger, should prevent inactivation. We find that this is indeed the case (Table I). When ubiquinol-cytochrome *c* reductase is treated with a 44 molar excess of hematoporphyrin and illuminated in the presence of 1 mM 2,5-dimethylfuran, only 12% inactivation is observed. Under the same conditions, but in the absence of dimethylfuran, a 98% inactivation is observed. The identity of singlet oxygen as the destructive agent is further substantiated by the failure of superoxide dismutase to protect photoinactivation (Table I). These results, together with the fact that illumination of hematoporphyrin generates singlet oxygen (Blum & Grossweiner, 1985), prove that singlet oxygen is indeed the destructive agent.

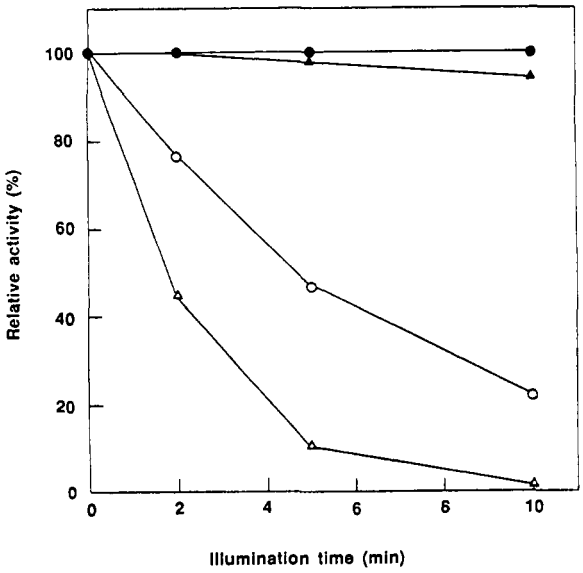

FIGURE 3: Hematoporphyrin-promoted photoinactivation of the intact and the Q- and phospholipid-depleted ubiquinol-cytochrome *c* reductases: 0.5-mL aliquots of intact, 0.60 μM cytochrome c_1 (○, ●) and Q- and PL-depleted, 0.61 μM cytochrome c_1 (△, ▲) reductases in 50 mM potassium phosphate buffer, pH 7.4, containing 0.25% sodium cholate in the presence (○, △) and absence (●, ▲) of 3 μM hematoporphyrin were illuminated under aerobic conditions. At the times indicated, aliquots were withdrawn and assayed for reductase activity. For illuminated intact enzyme, the activity was measured 10 min after standing at 0 °C in the dark; for illuminated depleted enzyme, the activity was measured after reconstitution with asolectin (0.2 mg/mg of protein) and incubation at 0 °C for 10 min. The 100% activity represents 15 and 10 μmol of cytochrome *c* reduced per minute per nanomole of cytochrome c_1 (at 23 °C) for intact and depleted reductases, respectively.

Effect of Ubiquinone on the Hematoporphyrin-Promoted Photoinactivation of Ubiquinol-Cytochrome c Reductase. Figure 3 compares the rates of hematoporphyrin-promoted photoinactivation of intact and Q- and phospholipid-depleted ubiquinol-cytochrome *c* reductases. The depleted enzyme, whose activity can be restored by reconstitution with Q and asolectin, exhibits a greater rate of photoinactivation than the intact enzyme. A 5-min illumination in the presence of a 3 molar excess of hematoporphyrin results in 53% and 89% inactivation for the intact and depleted reductases, respectively, suggesting that Q and/or phospholipids protect against photoinactivation.

Figure 4 shows the effect of Q_2 and Q_2H_2 on the hematoporphyrin-promoted photoinactivation of ubiquinol-cytochrome *c* reductase. Photoinactivation is significantly decreased when exogenous Q_2 or Q_2H_2 is present during illumination. In the presence of 25 μM Q_2 and Q_2H_2, inactivation is 45% and 38% as compared to the 98% inactivation without the addition of ubiquinone (Figure 4A). The protective effect of Q_2 and of Q_2H_2 on the hematoporphyrin-promoted photoinactivation of the reductase is Q_2 and Q_2H_2 concentration dependent (Figure 4B). The maximum protection is 45% and 60% for Q_2 and Q_2H_2, respectively.

Since both intact and delipidated ubiquinol-cytochrome *c* reductases are susceptible to photoinactivation, the protective effect of Q cannot be attributed solely to the Q–protein interaction. Other mechanisms must be considered. One way for Q to decrease photoinactivation might be by reaction with the generated singlet oxygen before it causes damage. Figure 2 shows that when hematoporphyrin is illuminated in the presence of Q_2H_2, the amount of nitroxide radical formed by 2,2,6,6-tetramethyl-4-piperidone is drastically decreased. However, the concentration of nitroxide radicals is not decreased if Q_2H_2 is added after illumination, indicating that ubiquinol does not react with nitroxide radicals; rather, it interacts with the generated singlet oxygen.

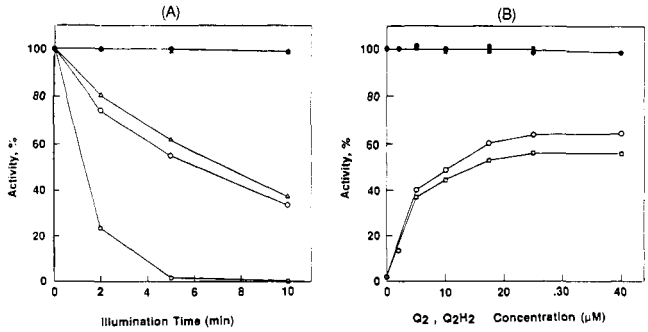

FIGURE 4: (A) Protective effect of ubiquinone-2 and ubiquinol-2 on the hematoporphyrin-promoted photoinactivation of ubiquinol-cytochrome *c* reductase. To 0.5-mL aliquots of ubiquinol-cytochrome *c* reductase, 0.3 μM cytochrome c_1, in 50 mM potassium phosphate buffer, pH 7.4, containing 0.25% sodium cholate in the presence (□, ○, △) and absence (●, ▲) of 15.2 μM hematoporphyrin was added 2.5 μL of 95% ethanolic solution cont ining no addition (□), 5 mM Q_2 (○, ●), or 5 mM Q_2H_2 (△, ▲) and subjected to illumination. At the times indicated, aliquots were withdrawn and assayed for ubiquinol-cytochrome *c* reductase activity. (B) Q_2 or Q_2H_2 concentration-dependent protection effect of the hematoporphyrin-promoted photoinactivation of ubiquinol-cytochrome *c* reductase. To 0.5-mL aliquots of ubiquinol-cytochrome *c* reductase, 0.47 μM cytochrome c_1, in 50 mM potassium phosphate buffer, pH 7.4, containing 0.25% sodium cholate in the presence (○, □) and absence (●, ■) of 15.2 μM hematoporphyrin were added the indicated concentrations of Q_2 (□, ■) of Q_2H_2 (○, ●) and illuminated for 5 min at room temperature. The 100% activity represents 15 μmol of cytochrome *c* reduced per minute per nanomole of cytochrome c_1 at 23 °C.

If quinone acts as a singlet oxygen scavenger, Q_2H_2 should be more effective than Q_2 in suppressing formation of nitroxide radicals because Q_2H_2 has a higher protective effect than Q_2 does. We find that this is indeed the case (Figure 4B). When hematoporphyrin is illuminated in the presence and absence of Q_2 or Q_2H_2, the amount of nitroxide radical decreased is slightly more with Q_2H_2 than with Q_2. The difference in scavenging effectiveness between Q_2H_2 and Q_2, however, is too small to account for the benzoquinone ring as the sold contributor; other parts of the ubiquinone molecule must also be involved, especially the double bonds in the alkyl side chain. The involvement of the double bonds was investigated by comparing the effectiveness of scavenger activity of Q_2 and its saturated side-chain derivative 2,3-dimethoxy-5-methyl-6-(3′,7′-dimethyloctyl)-1,4-benzoquinone. Both reduced and oxidized forms of 2,3-dimethoxy-5-methyl-6-(3′,7′-dimethyloctyl)-1,4-benzoquinone show only a partial (<20%) effectiveness of Q_2 in scavenging singlet oxygen. This result clearly establishes that the double bonds of the alkyl side chain of ubiquinone play an important role in scavenging singlet oxygen in addition to the benzoquinone ring.

That the protective effect of ubiquinone is not due to protein–ubiquinone interactions but to the singlet oxygen scavenger property of ubiquinone is further substantiated by the observation that ubiquinone protects against hematoporphyrin-promoted photoinactivation with other electron transfer complexes. When succinate-Q reductase or cytochrome *c* oxidase is illuminated for 10 min in the presence of a 44 molar excess hematoporphyrin, about 96% of the original activity is lost. However, when ubiquinone is present during illumination, the photoinactivation of succinate-ubiquinone reductase and cytochrome *c* oxidase is significantly decreased. Although one might argue that protection is due to protein–ubiquinone interactions in the case of succinate-ubiquinone reductase, this would seem unlikely for cytochrome *c* oxidase.

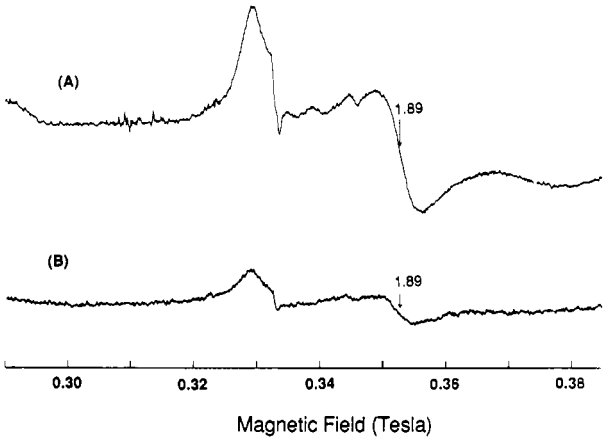

FIGURE 5: EPR spectra of iron–sulfur protein in the intact and photoinactivated ubiquinol-cytochrome *c* reductase. Aliquots of ubiquinol-cytochrome *c* reductases, 1.9 μM cytochrome c_1, containing 120 μM hematoporphyrin were kept in the dark (A) or illuminated for 5 min (B) at room temperature. Both the illuminated and control samples were precipitated by 40% saturation of ammonium sulfate and collected by centrifugation. The collected precipitates were dissolved in 50 mM potassium phosphate buffer, pH 7.4, containing 0.25% sodium cholate and 10 mM sodium ascorbate to a protein concentration of 22 mg/mL. EPR spectra were recorded at 80 K. The instrument settings were as follows: field modulation frequency, 100 kHz; microwave frequency, 9.34 GHz; modulation amplitude, 6.3 *g*; microwave power, 20 mW.

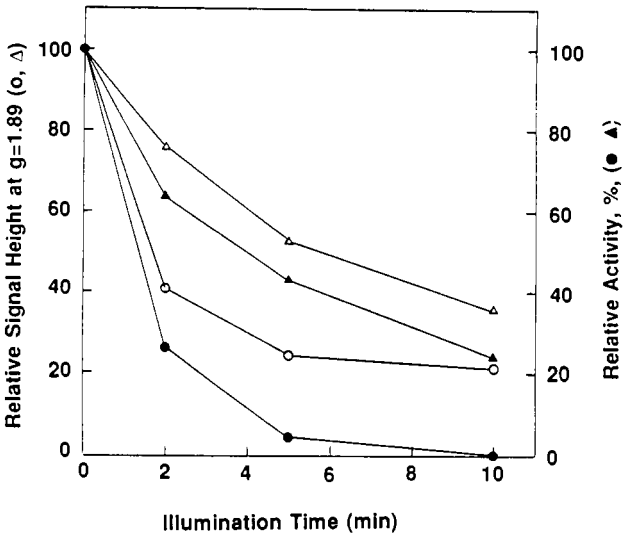

FIGURE 6: Correlation between the extent of photoinactivation and the EPR signal intensity of the iron–sulfur protein. Aliquots of ubiquinol-cytochrome *c* reductase, 1.9 μM cytochrome c_1, containing 91 μM hematoporphyrin in the presence (Δ, ▲) and absence (O, ●) of 69 μM Q_2 were subjected to illumination. At the times indicated, ubiquinol-cytochrome *c* reductase activity (●, ▲) and EPR spectra of iron–sulfur center (Δ, O) were determined. The reductase samples were concentrated for EPR measurements as described in Figure 5 after the activity was determined.

The singlet oxygen scavenger property of ubiquinone probably accounts for the protection.

The physiological significance of ubiquinone as a scavenger for singlet oxygen is difficult to determine at the present time. Since singlet oxygen can be generated during the oxidation of NADPH (King et al., 1975), the scavenger role of ubiquinone deserves more attention. We are currently investigating this aspect in our laboratory.

Characterization of Redox Components in Photoinactivated Ubiquinol-Cytochrome c Reductase. Ubiquinol-cytochrome *c* reductase contains five redox centers: two *b*-type cytochromes, one *c*-type cytochrome, Rieske's iron–sulfur cluster, and ubiquinone. It is important to know which of these components is modified or destroyed by singlet oxygen generated by hematoporphyrin. One way to locate the target site is to examine the properties of these redox components in photoinactivated reductase and compare them to those in normal samples.

Iron–Sulfur Clusters. When the EPR spectra of the iron–sulfur clusters in illuminated and unilluminated hematoporphyrin-treated ubiquinol-cytochrome *c* reductases are compared, a drastic decrease of $g = 1.89$ in EPR signal intensity is observed in photoinactivated reductase (Figure 5). The degree of iron–sulfur cluster destruction is proportional to the extent of inactivation, and Q_2, which protects against photoinactivation, also protects the iron–sulfur cluster (Figure 6). These results clearly indicate that the iron–sulfur cluster of Rieske's protein is the target site for the singlet oxygen. However, the possibility exists, though unlikely, that the observed decrease in the iron–sulfur cluster of photoinactivated reductase is secondary. To test this, reconstitutively active iron–sulfur protein prepared from ubiquinol-cytochrome *c* reductase by the method of Shimomura et al. (1986) was subjected to illumination in the presence and absence of hematoporphyrin. All of the $g = 1.89$ EPR signal is abolished upon illumination in the presence of hematoporphyrin, confirming that the iron–sulfur cluster of Rieske's protein is indeed the target site for the hematoporphyrin-promoted singlet oxygen. The fact that singlet oxygen causes no destruction to other redox centers of ubiquinol-cytochrome *c* reductase also indirectly supports the idea that the iron–sulfur cluster of Rieske's protein is the primary target site for hematoporphyrin-promoted photoinactivation.

Although the detailed mechanism for the destruction of the iron–sulfur cluster by singlet oxygen is not known, it is not likely due to the cleavage of the peptide bond of the apoprotein during photoinactivation because the SDS–PAGE pattern of the photoinactivated complex is identical with that of the intact complex. It is plausible to speculate that the oxidation of acid-labile sulfide, the cysteinyl, or the histidyl ligand of the cluster by the generated singlet oxygen is the cause of the destruction of the iron–sulfur cluster of Rieske's protein. The involvement of the histidyl ligand in Rieske's protein has recently been established (Cline et al., 1985; Telser et al., 1987; Gurbiel et al., 1989). The sulfide bond and the imidazol group are known to be susceptible to the singlet oxygen (Monroe, 1979; Kacher & Foote, 1979). The singlet oxygen oxidizes sulfide to sulfoxide. Since the treatment of photoinactivated ubiquinol-cytochrome *c* reductase with $FeCl_2$, Na_2S, and β-mercaptoethanol [a process known to generate an "artificial" iron–sulfur cluster from any protein which contains sulfhydryl groups (Yang & Huennekens, 1970)] does not restore the destroyed iron–sulfur cluster, the destruction of the iron–sulfur cluster of Rieske's protein by the singlet oxygen is not likely due to the oxidation of sulfide bonds. The comparison of the amino acid compositions of illuminated and of the unilluminated hematoporphyrin-treated pure iron–sulfur proteins and the comparison of amino acid composition of the iron–sulfur protein in the illuminated and the unilluminated hematoporphyrin-treated reductases (see Table II) reveal that one cysteinyl and two histidyl residues are destroyed, accompanied by the destruction of the iron–sulfur cluster by photoinactivation. The destruction of the iron–sulfur cluster of Rieske's protein by singlet oxygen results from the oxidation of these histidyl and cysteinyl groups. This result supports the recent finding that the nitrogen atom of the imidazole group of two histidines is involved in the ligation of the iron–sulfur cluster of Rieske's protein (Gurbiel et al., 1989). This result is also

Table II: Amino Acid Composition of Isolated and Photoinactivated Purified IS, ISP in Ubiquinol-Cytochrome c Reductase, and Ubiquinol-Cytochrome c Reductase[a]

	pure ISP (sequence data)		isolated ISP (mol %)		ISP in QCR (mol %)[b]		QCR (mol %)		
amino acid	residues	mol %	+hν	−hν	+hν	−hν	+hν	−hν	sequence data[c]
Asp (Asn)	16	8.10	8.16	8.08	8.64	8.22	8.41	8.39	7.95
Thr	9	4.59	4.80	4.62	4.50	4.60	5.01	5.01	5.11
Ser	19	9.69	9.25	9.47	9.90	10.09	6.97	6.95	7.72
Glu (Gln)	16	8.16	8.43	8.37	9.04	8.57	9.11	9.14	9.02
Pro	11	5.61	6.08	5.97	5.77	5.72	5.56	5.52	5.21
Gly	14	7.14	7.13	7.12	7.40	7.49	6.86	6.78	6.65
Ala	16	8.16	8.58	8.48	8.29	8.34	10.24	10.20	10.00
Val	19	9.69	9.66	9.32	9.25	9.10	6.96	6.92	7.07
Cys	4	2.04	1.38	1.91	1.35	1.81	1.10	1.20	1.26
Met	4	2.04	2.22	2.15	1.78	1.32	1.99	2.04	2.23
Ile	10	5.10	5.43	5.12	4.97	4.93	4.73	4.69	4.79
Leu	11	5.61	5.73	5.40	5.50	5.30	10.14	10.09	10.41
Tyr	7	3.57	4.20	4.02	3.86	3.72	3.91	3.89	3.81
Phe	7	3.57	3.40	3.46	3.91	3.77	4.52	4.59	4.51
Lys	15	7.65	7.30	7.27	7.23	7.02	4.92	4.95	5.11
His	6	3.06	1.75	3.11	2.31	3.38	2.84	3.05	2.88
Arg	10	5.10	5.48	5.16	5.27	5.00	5.42	5.32	5.16
Trp	2	1.02	nd	nd	nd	nd	nd	nd	1.26

[a] Mole percent of the amino acid residues except Trp was calculated on the basis of a total of 194 amino acid residues excluding Trp per mole of iron–sulfur protein as 98.98%. Mole percent of Cys was calculated on the basis of four residues per mole of iron–sulfur protein as 2.04%. Trp content was not determined. [b] ISP in QCR represents the iron–sulfur protein band sliced from the SDS-PAGE of ubiquinol-cytochrome c reductase. The protein in the gel slices was eluted electrophoretically. [c] Calculated from reported sequence data of all ten subunits of QCR, assuming that the amino acid composition of subunit I is similar to that of subunit II.

consistent with the observation that diethyl pyrocarbonate inhibits cytochrome b–c_1 complex at a site "phenomenologically" between cytochromes b and c_1 (Yagi et al., 1982).

The observation that hematoporphyrin-promoted singlet oxygen specifically destroys the cysteinyl and histidyl ligands of the iron–sulfur protein but not the ligands of cytochromes b (as described in the next section, little change in cytochrome b spectra is observed) can be explained by the lack of oxygen at, or the inaccessibility of hematoporphyrin to, the vicinity of the heme of cytochromes b. Since the generated singlet oxygen is not likely to travel a long distance, its target site is expected to be on or near its generation site. The Rieske's protein of ubiquinol-cytochrome c reductase has been shown to be located in a more hydrophilic environment (Schägger et al., 1987) than that of cytochrome b. The accessibility of hematoporphyrin to and the availability of oxygen at the iron–sulfur cluster make the latter a logical target site for singlet oxygen. The site-specific histidyl or cysteinyl residues destroyed by the hematoporphyrin-generated singlet oxygen are also reflected in the total amino acid composition (see Table II) of intact and photoinactivated ubiquinol-cytochrome c reductases. Besides the histidyl and cysteinyl residues, no significant change in the other amino acids is observed. Of these two changed amino acids, about 4 out of 62 histidyl residues and 2 or 3 out of 27 cysteinyl (or half-cystinyl) residues are destroyed in the photoinactivated reductase. The numbers of histidyl and cysteinyl residues in ubiquinol-cytochrome c reductase were calculated from the reported amino acid sequences of subunits I to X[2] (Anderson et al., 1981; Wakabayyashi et al., 1982a,b, 1985; Schägger et al., 1983, 1987; Brochart et al., 1985, 1986). The amino acid sequence or composition of subunit I is not yet available. It was assumed that the amino acid composition of subunit I is similar to that of subunit II.

A preparation of ubiquinol-cytochrome c reductase lacking only the iron–sulfur cluster is valuable in the study of electron transfer and proton translocation. This type of preparation has an advantage over the iron–sulfur protein depleted preparation since it has the intact protein structure of the complex. The role of the iron–sulfur cluster and its spatial relationship with other redox components can be established without complications due to conformational changes caused by the removal of the apoprotein of the iron–sulfur cluster. Since only the two histidyl residues involved in the ligating of the iron–sulfur cluster of Rieske's protein are destroyed, identification of these specific histidyl residues through conventional peptide analysis and amino acid sequencing will provide structural information about the iron–sulfur cluster. There are three histidyl residues located near the C-terminal end of Rieske's protein, but only two of them are involved in ligating the iron–sulfur cluster.

Cytochromes b and c_1. Figure 7 compares absorption characteristics of cytochromes c_1 (Figure 7A) and b (Figure 7B) in ubiquinol-cytochrome c reductase containing a 44-fold molar excess of hematoporphyrin with and without illumination. Cytochrome c_1 was measured by the difference spectra of ascorbate-reduced minus oxidized samples; cytochrome b was determined by the difference spectra of dithionite-reduced minus ascorbate-reduced samples. No significant decrease in the amount of cytochromes b and c_1 is observed after photoinactivation (less than 10% and 5% for cytochromes b and c_1, respectively). In the photoinactivated reductase, the α-absorption maximum for cytochrome c_1 remains unchanged, while the α-absorption peak for cytochrome b shows a 1-nm blue shift compared to the sample without illumination.

Although photoinactivation causes little change in the spectral characteristics of cytochromes b and c_1, a difference is observed in the rate of reduction of these cytochromes. The reduction of cytochrome b by $Na_2S_2O_4$ is more rapid in inactivated than in intact reductase (Figure 8A). About 96% of the cytochrome b in photoinactivated reductase is reduced in 10 s with 10 mM dithionite, compared to 69% in the intact sample. Although the rate of cytochrome b reduction by sodium dithionite in the photoinactivated complex is faster, the total dithionite-reducible cytochrome b in photoinactivated reductase is slightly less than that of intact reductase. The

[2] Unpublished data from our laboratory indicated that the active crystallized QCR contains only ten different subunits.

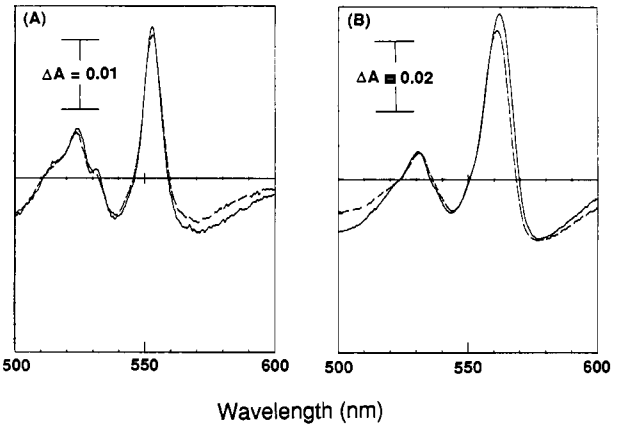

FIGURE 7: Difference spectra of the intact and photoinactivated ubiquinol-cytochrome *c* reductase. (A) Sodium ascorbate reduced minus oxidized form of intact (—) and of photoinactivated (--) ubiquinol-cytochrome *c* reductase; (B) sodium dithionite reduced minus sodium ascorbate reduced form of intact (—) and of photoinactivated (--) reductase. Photoinactivated reductase was prepared by illumination of a 2-mL aliquot of ubiquinol-cytochrome *c* reductase, 1.6 μM cytochrome c_1, in 50 mM potassium phosphate buffer, pH 7.4, containing 0.25% sodium cholate and 69.9 mM hematoporphyrin for 10 min at room temperature. Another identical sample without illumination was used as the intact sample. Oxidized, ascorbate-reduced, and dithionite-reduced samples were obtained by the addition of potassium ferricyanide (100 nmol), sodium ascorbate (20 μmol), and sodium dithionite (20 μmol), respectively.

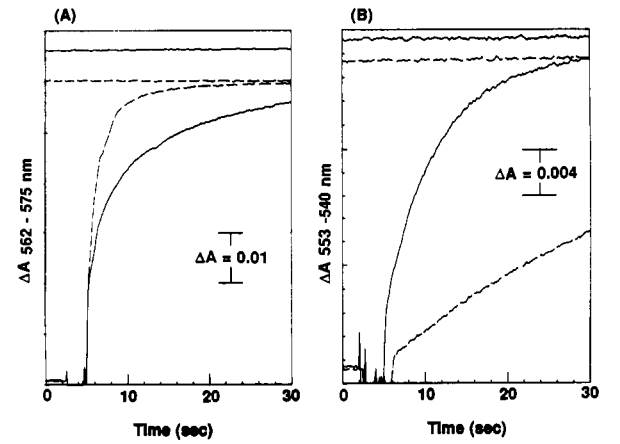

FIGURE 8: Reduction of cytochromes *b* and c_1 in the intact and the photoinactivated ubiquinol-cytochrome *c* reductases. The intact and photoinactivated ubiquinol-cytochrome *c* reductases were prepared as those given in Figure 3. Reduction of cytochromes *b* (A) and c_1 (B) was started by the addition of 20 μmol of sodium dithionite and 20 μmol of sodium ascorbate, respectively. The solid lines (—) are for the intact sample, and the broken lines (--) are for the photoinactivated sample. Upper horizontal lines in the figure indicate the full reduction level of each cytochrome.

reason for the change in the reduction rate is not known. It is possible that the destruction of the iron–sulfur cluster facilitates the access of $Na_2S_2O_4$ to cytochrome *b* and prevents the reduced cytochrome *b* from being reoxidized by the iron–sulfur cluster and subsequently by cytochrome c_1.

When succinate is added to reconstituted succinate-cytochrome *c* reductase formed from succinate-Q and ubiquinol-cytochrome *c* reductases, about 50% of total cytochrome *b* is reduced during the mixing time followed by a slow reduction of cytochrome *b*. When inactivated complex is reconstituted with succinate-Q reductase to form succinate-cytochrome *c* reductase (no succinate-cytochrome *c* reductase activity is observed), cytochrome *b* is reduced slowly when succinate is added. Thus the rapidly reduced cytochrome *b* component found in normal reconstituted succinate-cytochrome *c* reductase is missing when photoinactivated ubiquinol-cytochrome *c* reductase is used. The loss of rapidly reducible cytochrome *b* can be explained either by damage to the iron–sulfur cluster and that indirectly induced the conformation change of cytochrome *b* even though a direct contact between the iron–sulfur cluster and the heme moiety of cytochrome *b* has not been documented or by a minor modification of histidyl or cysteinyl residues of cytochrome *b* protein in photoinactivated reductase. It is also possible that the loss of rapidly reducible cytochrome *b* might be due to the destruction of one of the histidine ligands of cytochrome *b*. The minute change in the spectral properties of cytochrome *b*, the low degree of destruction of total histidine residues in reductase, and the lack of spectral modification of cytochrome c_1 in the photoinactivated reductase, however, lessens this possibility. Further characterization of cytochrome *b* is needed to answer this question.

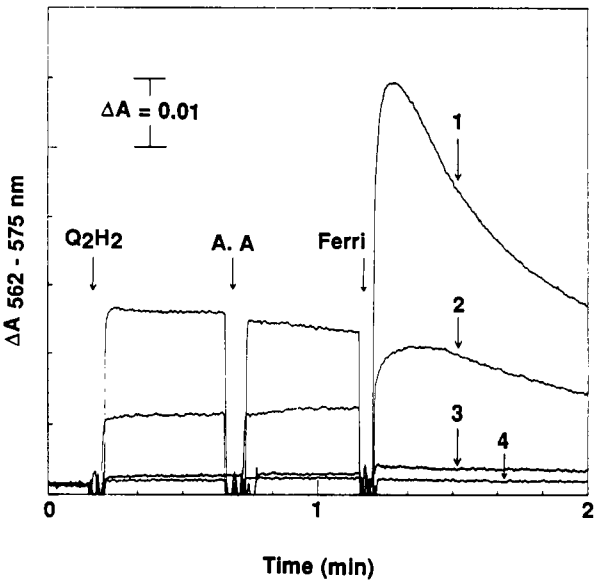

FIGURE 9: Photodynamic effect of hematoporphyrin on oxidant-induced reduction of cytochrome *b*: 2-mL aliquots of ubiquinol-cytochrome *c* reductase, 1.4 μM cytochrome c_1, in 50 mM potassium phosphate buffer, pH 7.4, containing 0.25% sodium cholate and 70.2 μM hematoporphyrin were illuminated for 0 (1), 2 (2), 5 (3), and 10 min (4). Q_2H_2 (144 nmol), antimycin A (25 nmol), and potassium ferricyanide (50 nmol) were added where indicated.

The rate of reduction of cytochrome c_1 by ascorbate (Figure 8B) in photoinactivated reductase is slower than in the intact sample. While 90% of the cytochrome c_1 in the intact reductase is reduced by 10 mM sodium ascorbate in 20 s, only 39% is reduced in the photoinactivated enzyme. This decrease in the reduction rate can be explained by the disruption of electron input to cytochrome c_1 through the iron–sulfur cluster. In other words, in the intact ubiquinol-cytochrome *c* reductase, ascorbate can reduce cytochrome c_1 directly or through the iron–sulfur protein, but in the photoinactivated reductase, cytochrome c_1 can only be reduced directly.

Q_2H_2 is known to partially reduce cytochrome *b* of ubiquinol-cytochrome *c* reductase in the presence and absence of antimycin (Zhu et al., 1983). In the presence of antimycin, the extent of cytochrome *b* reduction increases upon addition of oxidant, such as ferricyanide, a phenomenon generally known as oxidant-induced reduction of cytochrome *b* (Baum et al., 1967; Erecinska et al., 1972). Are these properties of cytochrome *b* affected by photoinactivation? Figure 9 compares the oxidant-induced cytochrome *b* reduction by intact and photoinactivated ubiquinol-cytochrome *c* reductases. In photoactivated reductase, the amount of cytochrome *b* reduced

by Q_2H_2 and the amount reduced by Q_2H_2 induced by ferricyanide in the presence of antimycin are much less than that reduced by intact samples. Furthermore, the decrease of oxidant-induced cytochrome *b* reduction in photoinactivated reductases is proportional to the extent of inactivation (data not shown). These results are consistent with the finding that hematoporphyrin-promoted photoinactivation of ubiquinol-cytochrome *c* reductase is due to damage of the iron–sulfur cluster of Rieske's protein, because the iron–sulfur cluster is thought to act as the first electron acceptor for ubiquinol oxidation (Mitchell, 1976; Yang, & Trumpower, 1988), thus generating a high reducing power in the transient ubisemiquinone radical that reduces cytochrome *b*. Without the iron–sulfur cluster, no ubisemiquinone radical will be generated; thus, no enhancement of cytochrome *b* reduction is expected.

Proton Translocation Activity of Photoinactivated Ubiquinol-Cytochrome c Reductase. In addition to the loss in activity, illumination of ubiquinol-cytochrome *c* reductase in the presence of hematoporphyrin also leads to the formation of a proton-leaking channel in the reductase. When the partially inactivated complex is incorporated in the photpholipid vesicles, no proton ejection is observed during the oxidation of ubiquinol (data not shown). Similarly, when photoinactivated complex is co-inlaid in vesicles with intact ubiquinol-cytochrome *c* reductase or cytochrome *c* oxidase, the proton ejection normally observed in the intact reductase or oxidase-inlaid vesicles is halted, suggesting that a proton-permeable channel is created in the photoinactivated ubiquinol-cytochrome *c* reductase whose iron–sulfur cluster is destroyed. The proton permeability of the reconstituted vesicles is not due to the presence of hematoporphyrin in the vesicles, because the intact ubiquinol-cytochrome *c* reductase vesicles formed in the presence of hematoporphyrin without prior illumination show normal proton ejection behavior. These results imply that, in addition to its essential role in electron transfer, the iron–sulfur cluster of Rieske's protein may participate in proton translocation. The ability of the photoinactivated ubiquinol-cytochrome *c* reductase to form proton-leaking phospholipid vesicles imbedded with electron transfer complexes provides a useful tool to study the fate of the localized and the bulk proton gradient in the oxidative phosphorylation. Work on this aspect is currently in progress in our laboratory.

Acknowledgments

We express our thanks to Dr. Roger Koeppe for critical review of the manuscript.

Registry No. Q, 606-06-4; O_2, 7782-44-7; hematoporphyrin, 14459-29-1; L-histidine, 71-00-1; ubiquinol–cytochrome *c* reductase, 9027-03-6.

References

Anderson, S. L., de Bruijin, M. H. L., Coulson, A. R., Eperson, I. C., Sanger, F., & Young, I. G. (1981) *J. Mol. Biol. 156*, 683–692.

Baum, H., Rieske, J. S., Sihman, H. J., & Lipton, S. H. (1967) *Proc. Natl. Acad. Sci. U.S.A. 57*, 798–805.

Bell, R. L., & Capaldi, R. A. (1976) *Biochemistry 15*, 996–1001.

Blum, A., & Grossweiner, L. I. (1985) *Photochem. Photobiol. 41*, 27–32.

Borchart, U., Machleidt, W. Schägger, H., Link, T. A., & von Jagow, G. (1985) *FEBS Lett. 191*, 125–130.

Borchart, U., Machleidt, W., Schägger, H., Link, T. A., & von Jagow, G. (1986) *FEBS Lett. 200*, 81–86.

Bourdon, J., & Durante, M. (1971) *Ann. N.Y. Acad. Sci. 171*, 163–174.

Cline, J. F., Hoffman, B. M., Mims, W. B., Lahaie, E., Ballou, D. P., & Fee, J. A. (1985) *J. Biol. Chem. 260*, 3251–3254.

Erecinska, M., Chance, B., Wilson, D. F., & Dutton, P. L. (1972) *Proc. Natl. Acad. Sci. U.S.A. 69*, 50–54.

Gellerfors, P., & Nelson, B. D. (1977) *Eur. J. Biochem. 80*, 275–282.

Gonzalez-Halphen, D., Lindorfer, M. A., & Capaldi, R. A. (1988) *Biochemistry 27*, 7021–7031.

Gurbiel, R. J., Batie, C. J., Sivaraja, M., True, A. E., Fee, J. A., Hoffman, B. M., & Ballou, D. P. (1989) *Biochemistry 28*, 4861–4871.

Hatefi, Y. (1985) *Annu. Rev. Biochem. 54*, 1015–1069.

Heinrikson, R. L., & Meredith, S. C. (1984) *Anal. Biochem. 136*, 65–74.

Hosokawa, Y., Suzuk, H., Toda, H., Nishikimi, M., & Ozawa, T. (1989) *J. Biol. Chem. 264*, 13483–13488.

Kacher, M. L., & Foote, C. S. (1979) *Photochem. Photobiol. 29*, 765–769.

Kagawa, Y., & Racker, E. (1971) *J. Biol. Chem. 246*, 5477–5487.

King, M. M., Lai, E. K., & McKay, P. B. (1975) *J. Biol. Chem. 250*, 6496–6502.

Laemmli, U. K. (1970) *Nature 227*, 680–685.

Mitchell, P. (1976) *J. Theor. Biol. 62*, 327–367.

Moan, J., & Wold, E. (1979) *Nature 279*, 450–451.

Monroe, B. M. (1979) *Photochem. Photobiol. 29*, 761–764.

Ninnemann, H., Butler, W. L., & Epel, B. L. (1970) *Biochim. Biophys. Acta 205*, 499–506.

Papa, S., Guerrieri, F., Lorusso, M., Izzo, G., & Capuano, F. (1982) in *Function of Quinones in Energy Conserving Systems* (Trumpower, B. L., Ed.) pp 527–539, Academic Press, New York.

Rieske, J. S. (1986) *J. Bioenerg. Biomembr. 18*, 235–257.

Schägger, H., von Jagow, G., Borchart, U., & Machleidt, W. (1983) *Hoppe-Seyler's Z. Physiol. Chem. 364*, 307–311.

Schägger, H., Link, T. A., Engel, W. D., & Von Jagow, G. (1986) *Methods Enzymol. 126*, 224–237.

Schägger, H., Borchart, U., Machleidt, W., Link, T. A., & Von Jagow, G. (1987) *FEBS Lett. 219*, 161–168.

Shimomura, Y., Nishikimi, M., & Ozawa, T. (1984) *J. Biol. Chem. 259*, 14059–14063.

Shimomura, Y., Nishikimi, M., & Ozawa, T. (1986) *Anal. Biochem. 153*, 126–131.

Spikes, J. D., & Macknight, M. L. (1971) *Ann. N.Y. Acad. Sci. 171*, 149–162.

Telser, J., Hoffman, B. M., Lobrutto, R., Ohnishi, T., Tsai, A.-L., Simpkin, D., & Palmer, G. (1987) *FEBS Lett. 214*, 117–121.

Trumpower, B. L., & Edwards, C. A. (1979) *J. Biol. Chem. 254*, 8697–8706.

Tsai, A.-L., Olson, J. S., & Palmer, G. (1987) *J. Biol. Chem. 262*, 8677–8684.

Von Jagow, G., & Link, T. A. (1986) *Methods Enzymol. 126*, 253–271.

Wakabayashi, S., Matsubara, H., Kim, C. H., & King, T. E. (1982a) *J. Biol. Chem. 259*, 9335–9344.

Wakabayashi, S., Takeda, H., Matsubara, H., Kim, C. H., & King, T. E. (1982b) *J. Biochem. (Tokyo) 91*, 2077–2085.

Wakabayashi, S., Takao, T., Shimonishi, Y., Kuramitsu, S., Matsubara, H., Wang, T. Y., Zhang, Z. P., & King, T. E. (1985) *J. Biol. Chem. 260*, 337–343.

Wikström, M., Krab, K., & Saraste, M. (1981) *Annu. Rev. Biochem. 50*, 623–655.

Yagi, T., Vik, S. B., & Hatefi, Y. (1982) *Biochemistry 21*, 4777-4782.
Yang, C. S., & Huennekens, F. M. (1970) *Biochemistry 9*, 2127-2133.
Yang, X., & Trumpower, B. L. (1988) *J. Biol. Chem. 263*, 11962-11970.
Yu, C. A., & Yu, L. (1980) *Biochemistry 19*, 5715-5720.
Yu, C. A., & Yu, L. (1982) *Biochemistry 21*, 4096-4101.
Yu, C. A., Yu, L., & King, T. E. (1974) *J. Biol. Chem. 249*, 4905-4910.
Zhu, Q. S., Van Der Wal, H. N., Van Grondelle, R., & Berden, J. A. (1983) *Biochim. Biophys. Acta 725*, 121-130.

Three-Dimensional Structure of *p*-Cresol Methylhydroxylase (Flavocytochrome *c*) from *Pseudomonas putida* at 3.0-Å Resolution†,‡

F. Scott Mathews,* Zhi-wei Chen, and Henry D. Bellamy§
Department of Cell Biology and Physiology, Washington University School of Medicine, St. Louis, Missouri 63110
William S. McIntire
Molecular Biology Division, Veterans Administration Medical Center, San Francisco, California 94121, and Department of Biochemistry and Biophysics and Department of Anesthesia, University of California, San Francisco, California 94143
Received January 19, 1990; Revised Manuscript Received August 31, 1990

ABSTRACT: *p*-Cresol methylhydroxylase (PCMH) isolated from *Pseudomonas putida* is an $\alpha_2\beta_2$ tetramer of approximate subunit M_r 49 000 and 9000. It is a flavocytochrome *c* containing covalently bound FAD in the larger subunit and covalently bound heme in the smaller. Crystals in space group $P2_12_12_1$ with unit-cell parameters a = 140.3 Å, b = 130.6 Å, and c = 74.1 Å contain one full molecule per asymmetric unit and diffract anisotropically to about 2.8-Å resolution in two directions and to about 3.3-Å resolution in the third. An electron density map has been computed at a nominal resolution of 3.0 Å by use of area detector data from native crystals and from two derivatives. The phases were improved with the B. C. Wang solvent leveling procedure, and the map was averaged about the noncrystallographic 2-fold axis. The cytochrome subunit, whose amino acid sequence is known, has been fitted to the electron density on a graphics system. The course of the polypeptide chain of the flavoprotein subunit, whose sequence is mostly unknown, has been traced in a minimap and a model of polyalanine fitted to the electron density on the graphics system. The flavoprotein subunit consists of three domains in close contact. The N-terminal domain consists largely of β-structure and contains most of the FAD binding site. The second domain contains a seven-stranded antiparallel β-sheet of unusual topology connected by antiparallel α-helices on one side. The flavin ring lies at the juncture of the first two domains. The third domain lies against the first domain and helps cover the rest of the FAD chain. The cytochrome subunit resembles other small cytochromes such as *c*-551 and c_5 and fits into a depression on the surface of the large flavoprotein subunit. The flavin and heme planes are nearly perpendicular, the normals to the planes being approximately 65° apart. The two groups are separated by about 8 Å, the distance from one of the vinyl methylene carbon atoms of the heme to the 8α-methyl group of the flavin ring.

p-Cresol methylhydroxylase (PCMH)[1] is a flavocytochrome *c* found in the periplasmic space of certain pseudomonads. It catalyzes the first steps in the oxidation of *p*-cresol to *p*-hydroxybenzaldehyde (Hopper & Taylor, 1977). The product is then converted to *p*-hydroxybenzoic acid and subsequently undergoes ring fission in later catalytic steps. During catalysis, hydroxylation of *p*-cresol occurs by the abstraction of two hydrogen atoms by the flavoprotein after which the putative *p*-quinone methide intermediate is believed to be attacked by water to yield *p*-hydroxybenzyl alcohol (Hopper, 1976). The two electrons are then transferred one at a time to the heme on the cytochrome subunit and then to an acceptor protein in vivo (Hopper, 1978). The acceptor protein is believed to be an azurin (McIntire et al., 1985). The product of the reaction, *p*-hydroxybenzyl alcohol, can also serve as substrate for the enzyme in a dehydrogenation reaction yielding *p*-hydroxybenzaldehyde. In vitro, phenazine methosulfate can act as an artificial electron acceptor for the protein.

Seven forms of PCMH have been isolated from six bacterial sources (Koerbert et al., 1985; Bossert et al., 1989). A flavocytochrome *c* preferring 4-ethylphenol as its primary substrate, and which is closely related to PCMH, has also recently been characterized (Reeves et al., 1989). *Pseudomonas putida* strain NCIB 9869 produces two forms of PCMH (Keat & Hopper, 1978). One, form A, is carried on a plasmid and is expressed constitutively by cells grown on 3,5-xylenol. The other, form B, is chromosomally encoded and is induced by *p*-cresol. PCMH form A, the subject of this study, has a molecular weight of approximately 116000. It can be resolved

† This work has been supported by NSF Grants DMB-8816618 and DMB-8718741, USPHS Grant HL-16251, and the Veterans Administration.
‡ Crystallographic coordinates for PCMH have been submitted to the Brookhaven Protein Data Bank.
* Corresponding author.
§ Present address: Stanford Synchrotron Radiation Laboratory, SLAC Bin 69, P.O. Box 4349, Stanford, CA 94309.

[1] Abbreviations: PCMB, *p*-(chloromercuri)benzoate; PCMH, *p*-cresol methylhydroxylase; PEG, poly(ethylene glycol); rms, root mean square.

0006-2960/91/0430-238$02.50/0